

Posterior Mode Guided Dimension Reduction for Bayesian Model Averaging in Heavy-Tailed Linear Regression

Shamriddha De* and Joyee Ghosh†

Abstract

For large model spaces, the potential entrapment of Markov chain Monte Carlo (MCMC) based methods with spike-and-slab priors poses significant challenges in posterior computation in regression models. On the other hand, maximum a posteriori (MAP) estimation, which is a more computationally viable alternative, fails to provide uncertainty quantification. To address these problems simultaneously and efficiently, this paper proposes a hybrid method that blends MAP estimation with MCMC-based stochastic search algorithms within a heavy-tailed error framework. Under hyperbolic errors, the current work develops a two-step expectation conditional maximization (ECM) guided MCMC algorithm. In the first step, we conduct an ECM-based posterior maximization and perform variable selection, thereby identifying a reduced model space in a high posterior probability region. In the second step, we execute a Gibbs sampler on the reduced model space for posterior computation. Such a method is expected to improve the efficiency of posterior computation and enhance its inferential richness. Through simulation studies and benchmark real life examples, our proposed method is shown to exhibit several advantages in variable selection and uncertainty quantification over various state-of-the-art methods.

Keywords: Bayesian variable selection, Expectation Conditional Maximization (ECM), Hyperbolic distribution, Markov chain Monte Carlo (MCMC), Maximum a posteriori (MAP) estimation, Spike-and-slab priors.

1 Introduction

The extensive literature on variable selection in linear regression models spans a broad range of modeling techniques, ranging from the classical formulations based on normal errors to more recent approaches that emphasize robustness to departures from normality. From a Bayesian point

*PhD Candidate, Department of Statistics and Actuarial Science, The University of Iowa, Iowa City, USA

†Associate Professor, Department of Statistics and Actuarial Science, The University of Iowa, Iowa City, USA

of view, the problem of variable selection is often addressed by putting spike-and-slab priors on the regression coefficients. Several authors, including [George and McCulloch \(1993, 1997\)](#); [Gramacy and Pantaleo \(2010\)](#); [Hans \(2010, 2011\)](#); [Clyde et al. \(2011\)](#); [Ghosh and Clyde \(2011\)](#); [Ghosh and Ghattas \(2015\)](#); [Zanella and Roberts \(2019\)](#); [Nie and Ročková \(2023a\)](#), have utilized such priors to incorporate model uncertainty under normal error models. Spike-and-slab prior formulations have also been adopted for Bayesian variable selection and model averaging in linear regression models with heavy-tailed errors ([Gramacy and Pantaleo, 2010](#); [Ren et al., 2023](#); [Chakraborty et al., 2025](#); [De and Ghosh, 2026](#)).

Under spike-and-slab priors, the size of the model space grows exponentially with the number of predictors. Thus, even a modest increase in the number of predictors results in a large model space, whose posterior exploration with Markov chain Monte Carlo (MCMC) is computationally daunting. Owing to the multimodal structure of the posterior distribution, standard MCMC algorithms are susceptible to entrapment at local modes. Rather than full posterior exploration, a more viable alternative is to focus on the restricted goal of posterior mode estimation, commonly referred to as maximum a posteriori (MAP) estimation. The availability of non-stochastic maximization techniques like the expectation maximization (EM) algorithm and its variants ([Dempster et al., 1977](#); [Meng and Rubin, 1993](#); [Wei and Tanner, 1990](#); [Ruth, 2024](#)) has further inspired many authors to explore and implement efficient MAP-based techniques. In particular, [Ročková and George \(2014\)](#) proposed the expectation maximization variable selection (EMVS) algorithm with continuous spike-and-slab priors in a normal error model. For the normal likelihood, [Ročková and George \(2018\)](#) later proposed the spike-and-slab lasso by combining spike-and-slab priors with the Bayesian lasso using Laplace priors ([Park and Casella, 2008](#)) on the regression coefficients. A more robust version of the spike-and-slab lasso with asymmetric Laplace errors was recently developed by [Liu et al. \(2024\)](#) through the spike-and-slab quantile lasso (SSQLASSO).

Despite a significant computational gain over MCMC algorithms, deterministic MAP-based methods in the literature have primarily focused on coefficient estimation and variable selection. They lack uncertainty quantification for tail heaviness estimation, which is a core objective of pos-

terior sampling via MCMC methods. In other words, neither MCMC nor MAP-based methods can typically provide a stand-alone pathway to all the aforementioned goals in high-dimensional regression models with potentially heavy-tailed errors. Motivated by this limitation, we try to simultaneously address both computational efficiency and inferential richness within a flexible modeling framework by blending MAP estimation with MCMC-based stochastic search algorithms. For this purpose, we model the errors using the hyperbolic distribution and propose a two-step expectation conditional maximization (ECM) algorithm (Meng and Rubin, 1993) guided MCMC framework. The hyperbolic error model (HEM) ensures flexibility in tail heaviness by typically varying its shape parameter η . In the first step of our proposed method, for a suitably chosen degree of tail heaviness (fixed value of η), we conduct an ECM-based posterior maximization and perform variable selection using spike-and-slab priors on the regression coefficients. The tail heaviness parameter η is treated as fixed at this stage, as ECM-based estimation of tail heaviness is often inaccurate. This approach efficiently identifies a reduced model space in a high posterior density region, based on the chosen predictors. The second step is inspired by a special case of the stochastic search variable selection approach of De and Ghosh (2026). More specifically, in the second step, we implement a Gibbs sampler with a Metropolis-Hasting step on the reduced model space, and perform posterior inference for tail thickness by putting a prior on η . We use the shorthand GE_{CM}-HEM to denote our proposed ECM guided Gibbs (G) sampling algorithm for the hyperbolic error model (HEM).

The rest of the article is organized as follows. In Section 2, we introduce our proposed two-step GE_{CM}-HEM algorithm. In Section 3, we carry out a simulation study to compare the performance of our proposed method with the stochastic search HEM (De and Ghosh, 2026), as well as with two other state-of-the-art MAP estimation techniques. We analyze three real life datasets in Section 4. Concluding remarks and possible directions for future work are stated in Section 5. The proof of a proposition pertaining to the normal scale mixture representation of the hyperbolic distribution is outlined in Appendix A. Some additional results for one of the real datasets (Ames Housing dataset) are reported in Appendix B. For clarity on parameterization, the probability density func-

tions of some distributions used in the article are provided in Appendix C.

2 The GECM Approach Towards the Hyperbolic Error Model

We begin this section by briefly revisiting the hyperbolic error model (HEM) (De and Ghosh, 2026) implemented with MCMC, which serves as a precursor to our proposed method. Thereafter, we describe our proposed technique and discuss the suggested choices for the relevant hyperparameters in detail.

2.1 Review of the Stochastic Search Hyperbolic Error Model

To induce flexibility in tail heaviness, De and Ghosh (2026) proposed a mixture of the hyperbolic and the Student- t distributions for modeling the errors, and showed that this mixture model reduces to the HEM as a special case. Given the pivotal role of the HEM in the present paper, we review it at the outset.

Let us consider a linear regression model

$$\mathbf{Y} = X\boldsymbol{\beta} + \boldsymbol{\epsilon}, \quad (1)$$

with an $n \times 1$ response vector \mathbf{Y} , an $n \times p$ design matrix X of p covariates, $\boldsymbol{\beta}$ as the $p \times 1$ vector of unknown regression coefficients, and $\boldsymbol{\epsilon}$ as the n -dimensional vector of independent and identically distributed hyperbolic errors. More precisely, the error distribution has the form

$$f_{\text{Hyperbolic}}(\epsilon_i | \eta, \rho^2) = \frac{1}{2\sqrt{\eta\rho^2}K_1(\eta)} e^{-\{\eta(\eta + \epsilon_i^2/\rho^2)\}^{1/2}}, \quad -\infty < \epsilon_i < \infty, \quad i = 1, 2, \dots, n, \quad (2)$$

with shape parameter $\eta > 0$ and scale parameter $\rho^2 > 0$. Including an intercept term in (1) is redundant, since the covariates and the response variables are centered and scaled about their respective means and standard deviations. The model uncertainty in (1) is introduced using a p -dimensional latent binary vector $\boldsymbol{\gamma} = (\gamma_1, \gamma_2, \dots, \gamma_p)^\top$, where $\gamma_j \in \{0, 1\}$, for every $j = 1, 2, \dots, p$, with

$\gamma_j = 0$ and $\gamma_j = 1$ respectively signifying the exclusion or inclusion of the j th covariate in the model. For every model γ in the model space $\Gamma = \{0, 1\}^p$, we define β_γ to be the p_γ -dimensional vector of the non-zero components in β , where $p_\gamma = \sum_{j=1}^p \gamma_j$, and let X_γ denote the matrix of the corresponding columns of the design matrix X .

[Gneiting \(1997\)](#) expressed the hyperbolic density as a normal scale mixture with a generalized inverse Gaussian (GIG) mixing density, which has been utilized by [Park and Casella \(2008\)](#); [De and Ghosh \(2024, 2026\)](#) to formulate a computationally efficient likelihood for model (1). The said likelihood, along with the hierarchical prior specification by [De and Ghosh \(2026\)](#) for the unknown parameters, are stated below:

$$\begin{aligned}
\mathbf{Y}|\boldsymbol{\gamma}, \boldsymbol{\beta}, \boldsymbol{\sigma} &\sim \text{N}(X_\gamma \boldsymbol{\beta}_\gamma, \Sigma), \\
\sigma_i^2|\rho^2, \eta &\stackrel{\text{ind}}{\sim} \text{GIG}(1, \eta/\rho^2, \eta\rho^2), \quad i = 1, 2, \dots, n, \\
\beta_j|\gamma_j, \rho^2, \tau^2 &\stackrel{\text{ind}}{\sim} \text{N}(0, \rho^2\tau^2) \mathbb{I}(\gamma_j = 1) + \delta_{\{0\}}(\beta_j) \mathbb{I}(\gamma_j = 0), \quad j = 1, 2, \dots, p, \\
\tau^2 &\sim \text{InvGamma}(\lambda_\tau/2, \lambda_\tau/2), \\
\rho^2 &\sim \text{InvGamma}(a_\rho, b_\rho), \\
\eta &\sim \text{DiscUniform}(\mathcal{G}_\eta), \\
\gamma_j|\theta &\stackrel{\text{ind}}{\sim} \text{Bernoulli}(\theta), \quad j = 1, 2, \dots, p, \\
\theta &\sim \text{Beta}(c_\theta, d_\theta), \tag{3}
\end{aligned}$$

where $\boldsymbol{\sigma} = (\sigma_1^2, \sigma_2^2, \dots, \sigma_n^2)^\top$, $\Sigma = \text{diag}(\sigma_1^2, \sigma_2^2, \dots, \sigma_n^2)$, $\lambda_\tau > 0$, $a_\rho > 0$, $b_\rho > 0$, $c_\theta > 0$, $d_\theta > 0$, \mathcal{G}_η is a finite set of positive real numbers, $\delta_{\{0\}}(\cdot)$ represents a point mass at zero, and $\mathbb{I}(\cdot)$ denotes the indicator function. Armed with these priors and likelihood, [De and Ghosh \(2026\)](#) developed a Gibbs sampler with a Metropolis-Hastings step for posterior computation. As far as the prior support \mathcal{G}_η of η is concerned, [De and Ghosh \(2024, 2026\)](#) recommended $\mathcal{G}_\eta = \{0.05, 0.1, 0.2, 0.3, \dots, 0.9, 1, 2, 5, 10, 20, 50\}$ as a suitable grid encompassing a wide range of tail heaviness.

While the stochastic search HEM can be viewed as a gold standard for model averaging in

a heavy-tailed framework, computational challenges emerge in problems involving large model spaces. The multimodal nature of the posterior distribution over the models often causes the Gibbs sampler to get trapped in local modes. Escaping such entrapment demands the execution of extremely long chains of the sampler and compromises the computational efficiency of the algorithm. Resorting to a simplified goal of MAP estimation through EM-like algorithms appears to be a more practical alternative to address the drawbacks of the stochastic search HEM. However, the lack of uncertainty quantification in such deterministic techniques highlights the continued need for the Gibbs sampler. Accordingly, we propose an algorithm that combines the computational efficiency of deterministic MAP estimation with the uncertainty quantification provided by stochastic search MCMC.

2.2 The ECM Guided Gibbs Sampling

We develop a two-step method that combines deterministic MAP estimation for computational speed with stochastic search MCMC for uncertainty quantification, particularly in the tails, thereby leveraging the complementary strengths of both the approaches. Our proposed technique begins with an initial level of variable selection based on posterior mode estimation via the ECM algorithm (Meng and Rubin, 1993), followed by a Gibbs sampler that performs a final level of variable selection on the reduced model space obtained from the modal estimates.

Step 1: The ECM Step

In the first step, we intend to estimate the mode of the posterior distribution, marginalized over the model uncertainty parameter γ , that is, $p(\beta, \rho^2, \eta, \theta, \tau^2, \sigma | \mathbf{Y}) = \sum_{\gamma} p(\gamma, \beta, \rho^2, \eta, \theta, \tau^2, \sigma | \mathbf{Y})$. However, for a large value of p , direct maximization through complete enumeration of all the 2^p models and taking summation over them is computationally infeasible. Therefore, following Ročková and George (2014), we consider γ as the “missing data” and maximize the conditional expectation of the “complete data” log-posterior $\log p(\gamma, \beta, \rho^2, \eta, \theta, \tau^2, \sigma | \mathbf{Y})$. The conditional expectation is taken over γ , given the observed data \mathbf{Y} and the current parameter estimates. Due to

the unavailability of closed-form expressions for simultaneous maximization for all the parameters, the ECM algorithm (Meng and Rubin, 1993) is applied to maximize over blocks of parameters conditionally on others.

For computational ease in the ECM step, we make a few changes to (3). A slightly modified version of the scale mixture representation of the hyperbolic distribution by Gneiting (1997) is indicated in Proposition 1 and is proven in Appendix A.

Proposition 1. *Let A and a be random variables such that $A|a^2 \sim N(0, \rho^2 a^2)$ and $a^2 \sim \text{GIG}(1, \eta, \eta)$. Then A is distributed as $\text{Hyperbolic}(\eta, \rho^2)$.*

The scale mixture representation in Proposition 1 leads to the following reformulated likelihood for model (1), which has been deployed in the ECM step:

$$\begin{aligned} \mathbf{Y}|\boldsymbol{\beta}, \boldsymbol{\sigma}, \rho^2 &\sim N(X\boldsymbol{\beta}, \rho^2\Sigma), \\ \sigma_i^2|\eta &\stackrel{\text{ind}}{\sim} \text{GIG}(1, \eta, \eta), \quad i = 1, 2, \dots, n. \end{aligned} \tag{4}$$

Moreover, to ensure differentiability of the objective function, we replace the mixture of point mass at zero and a continuous prior (point mass spike-and-slab prior) on the regression coefficients by a continuous spike-and-slab prior. That is, we consider a mixture of two continuous distributions as the prior, where one component (spike) is concentrated around zero, while the other component (slab) is more diffuse. Such a prior shrinks the coefficients for the noise variables towards zero, but cannot enforce them to be exactly zero. Therefore, the modal estimate of $\boldsymbol{\beta}$ does not explicitly drop any covariate from the model. For the remaining parameters $\boldsymbol{\gamma}$, ρ^2 , τ^2 and θ , we retain the

priors in (3). In a nutshell, the priors used for the ECM step are stated below:

$$\begin{aligned}
\beta_j | \gamma_j, \rho^2, \tau^2 &\stackrel{\text{ind}}{\sim} (1 - \gamma_j)N(0, \kappa_0 \rho^2 \tau^2) + \gamma_j N(0, \kappa_1 \rho^2 \tau^2), \quad j = 1, 2, \dots, p, \\
\tau^2 &\sim \text{InvGamma}(\lambda_\tau/2, \lambda_\tau/2), \\
\rho^2 &\sim \text{InvGamma}(a_\rho, b_\rho), \\
\eta &\sim \text{DiscUniform}(\mathcal{G}_\eta), \\
\gamma_j | \theta &\stackrel{\text{ind}}{\sim} \text{Bernoulli}(\theta), \quad j = 1, 2, \dots, p, \\
\theta &\sim \text{Beta}(c_\theta, d_\theta),
\end{aligned} \tag{5}$$

where $\kappa_0 > 0$ and $\kappa_1 > 0$ are respectively chosen to be small and large, corresponding to the spike and the slab components. The hyperparameters κ_0 and κ_1 control the strengths of the respective spike and slab components. A smaller value of κ_0 indicates a more peaked spike with more concentration around zero, while a larger value of κ_1 signifies a flatter slab.

Preliminary analyses of the ECM algorithm revealed poor estimation of the tail heaviness for modest sample size or weak signal strength, under the priors in (5). Accordingly, instead of maximizing with respect to the shape parameter η over its prior support \mathcal{G}_η , we fix its value at $\eta = 1$, corresponding to a slightly heavier tail than the normal distribution. This strategy tends to provide some safeguard against the potential adversities of variable selection under a misspecified light-tailed model.

Let $\mathbb{E}_\gamma^*[\cdot]$ denote the conditional expectation $\mathbb{E}_\gamma[\cdot | \mathbf{Y}, \eta = 1, \hat{\boldsymbol{\beta}}, \hat{\rho}^2, \hat{\theta}, \hat{\tau}^2, \hat{\boldsymbol{\sigma}}]$ over $\boldsymbol{\gamma}$, given \mathbf{Y} , $\eta = 1$, and the current estimates $\hat{\boldsymbol{\beta}}$, $\hat{\rho}^2$, $\hat{\theta}$, $\hat{\tau}^2$ and $\hat{\boldsymbol{\sigma}}$ of the remaining parameters $\boldsymbol{\beta}$, ρ^2 , θ , τ^2 and $\boldsymbol{\sigma}$ respectively. The goal is to maximize the conditional expectation $\mathbb{E}_\gamma^*[\log p(\boldsymbol{\gamma}, \boldsymbol{\beta}, \rho^2, \theta, \tau^2, \boldsymbol{\sigma})]$, which, using the likelihood and the priors in (4) and (5), reduces to iteratively maximizing the

function

$$\begin{aligned}
Q = & -\frac{1}{2} \left\{ n \log \rho^2 + (1 + \eta) \sum_{i=1}^n \sigma_i^2 + \frac{1}{\rho^2} (\mathbf{Y} - X\boldsymbol{\beta})^\top \Sigma^{-1} (\mathbf{Y} - X\boldsymbol{\beta}) + \eta \sum_{i=1}^n \frac{1}{\sigma_i^2} + 2n \log K_1(\eta) \right\} \\
& - \frac{1}{2} \left\{ \sum_{j=1}^p \mathbb{E}_\gamma^*[\log \alpha_j] + p \log \rho^2 + \frac{1}{\rho^2 \tau^2} \boldsymbol{\beta}^\top \Omega \boldsymbol{\beta} + (p + \lambda_\tau + 2) \log \tau^2 + \frac{\lambda_\tau}{\tau^2} \right\} \\
& - \left\{ (a_\rho + 1) \rho^2 + \frac{b_\rho}{\rho^2} \right\} + (p + d_\theta - 1) \log(1 - \theta) + (c_\theta - 1) \log \theta + \log \left(\frac{\theta}{1 - \theta} \right) \sum_{j=1}^p \mathbb{E}_\gamma^*[\gamma_j],
\end{aligned} \tag{6}$$

where $\eta = 1$, $\alpha_j = \kappa_0(1 - \gamma_j) + \kappa_1\gamma_j$ for $j = 1, 2, \dots, p$, and $\Omega = \text{diag}((\mathbb{E}_\gamma^*[1/\alpha_j]))$. The complicated nature of the objective function Q prohibits closed-form maximization to be performed jointly over all the parameters using the traditional EM algorithm (Dempster et al., 1977). As an alternative, we adopt the ECM algorithm (Meng and Rubin, 1993), which proceeds by maximizing Q sequentially over each parameter, conditional on the current estimates of the remaining parameters.

1. **The E-Step:** In the expectation (E) step, we compute the conditional expectations $\mathbb{E}_\gamma^*[\gamma_j]$, $\mathbb{E}_\gamma^*[\log \alpha_j]$ and $\mathbb{E}_\gamma^*[1/\alpha_j]$, for every $j = 1, 2, \dots, p$. We note that the conditional posterior distribution of γ , given the response variables \mathbf{Y} , $\eta = 1$ and the current estimates $(\hat{\boldsymbol{\beta}}, \hat{\rho}^2, \hat{\theta}, \hat{\tau}^2, \hat{\boldsymbol{\sigma}})$, depends on $(\mathbf{Y}, \eta = 1, \boldsymbol{\sigma})$ only through $(\hat{\boldsymbol{\beta}}, \hat{\rho}^2, \hat{\theta}, \hat{\tau}^2)$, and the conditional expectation $\mathbb{E}_\gamma^*[\gamma_j]$ simplifies to

$$\mathbb{E}_\gamma^*[\gamma_j] = \mathbb{P}(\gamma_j = 1 | \mathbf{Y}, \eta = 1, \hat{\boldsymbol{\beta}}, \hat{\rho}^2, \hat{\theta}, \hat{\tau}^2, \hat{\boldsymbol{\sigma}}) = \frac{p(\hat{\beta}_j | \gamma_j = 1, \hat{\rho}^2, \hat{\tau}^2) \mathbb{P}(\gamma_j = 1 | \hat{\theta})}{\sum_{t=0}^1 p(\hat{\beta}_j | \gamma_j = t, \hat{\rho}^2, \hat{\tau}^2) \mathbb{P}(\gamma_j = t | \hat{\theta})} = g_j, \tag{7}$$

for every $j = 1, 2, \dots, p$. The prior specification in (5) ensures computational tractability of the quantities involved in (7). Furthermore, for every $j = 1, 2, \dots, p$, the remaining conditional expectations can be evaluated using (7) as weighted averages of functions of the

spike and the slab strength hyperparameters κ_0 and κ_1 in the following manner:

$$\begin{aligned}\mathbb{E}_\gamma^*[\log \alpha_j] &= \mathbb{E}_\gamma^*[\log \{\kappa_0(1 - \gamma_j) + \kappa_1\gamma_j\}] = (1 - g_j) \log \kappa_0 + g_j \log \kappa_1, \\ \mathbb{E}_\gamma^*[1/\alpha_j] &= \mathbb{E}_\gamma^*\left[\frac{1}{\kappa_0(1 - \gamma_j) + \kappa_1\gamma_j}\right] = \frac{1 - g_j}{\kappa_0} + \frac{g_j}{\kappa_1}.\end{aligned}\quad (8)$$

2. **The CM-Step:** The conditional maximization (CM) step of the ECM algorithm maximizes the objective function Q for each parameter, given the current estimates of the remaining parameters, and yields the following closed-form estimates at every iteration:

$$\begin{aligned}\hat{\boldsymbol{\beta}} &= \left(X^\top \hat{\Sigma}^{-1} X + \frac{1}{\hat{\tau}^2} \Omega\right)^{-1} X^\top \hat{\Sigma}^{-1} \mathbf{Y}, \\ \hat{\rho}^2 &= \frac{2b_\rho + (\mathbf{Y} - X\hat{\boldsymbol{\beta}})^\top \Sigma^{-1} (\mathbf{Y} - X\hat{\boldsymbol{\beta}}) + \hat{\boldsymbol{\beta}}^\top \Omega \hat{\boldsymbol{\beta}} / \hat{\tau}^2}{n + p + 2a_\rho + 2}, \\ \hat{\tau}^2 &= \frac{\lambda_\tau + \hat{\boldsymbol{\beta}}^\top \Omega \hat{\boldsymbol{\beta}} / \hat{\rho}^2}{p + \lambda_\tau + 2}, \\ \hat{\theta} &= \frac{c_\theta + \sum_{j=1}^p g_j - 1}{c_\theta + d_\theta + p - 2}, \\ \hat{\sigma}_i^2 &= \frac{1}{2\eta} \left[-1 + \left\{ 1 + 4\eta \left(\eta + \frac{(y_i - \mathbf{x}_i^\top \hat{\boldsymbol{\beta}})^2}{\hat{\rho}^2} \right) \right\}^{1/2} \right], \quad i = 1, 2, \dots, n,\end{aligned}\quad (9)$$

where $\eta = 1$, $\hat{\Sigma} = \text{diag}(\hat{\sigma}_1^2, \hat{\sigma}_2^2, \dots, \hat{\sigma}_n^2)$, and for every $i = 1, 2, \dots, n$, \mathbf{x}_i is the i th row of the design matrix X and y_i is the i th component of the response vector \mathbf{Y} .

Under continuous spike-and-slab priors, the modal estimates of the regression coefficients cannot be exactly zero and therefore do not allow explicit exclusion of a covariate. Moreover, the median probability model (Barbieri and Berger, 2004) and other Bayes factor based approaches (Ghosh and Ghattas, 2015; De and Ghosh, 2026), which rely on thresholding the posterior probability $\mathbb{P}(\gamma_j = 1 | \mathbf{Y})$ to select covariates, are not applicable here because the posterior distribution over models is unavailable.

Ročková and George (2014) estimated the most probable submodel as the highest probability model conditional on the modal estimates of the parameters. Following this strategy, we choose

our best submodel as the model with the highest conditional probability, given $\eta = 1$ and the modal estimates $(\hat{\beta}, \hat{\rho}^2, \hat{\theta}, \hat{\tau}^2, \hat{\sigma})$ from the ECM algorithm. That is, the estimated model is

$$\hat{\gamma} = \arg \max_{\gamma} \mathbb{P}(\gamma | \eta = 1, \hat{\beta}, \hat{\rho}^2, \hat{\theta}, \hat{\tau}^2, \hat{\sigma}), \quad (10)$$

which can be obtained by thresholding the conditional probability of each component as

$$\hat{\gamma}_j = 1 \quad \iff \quad \mathbb{P}(\gamma_j = 1 | \eta = 1, \hat{\beta}, \hat{\rho}^2, \hat{\theta}, \hat{\tau}^2, \hat{\sigma}) \geq 0.5, \quad (11)$$

for every $j = 1, 2, \dots, p$. In other words, the j th covariate is dropped from our model if the conditional probability of the corresponding ‘‘slab’’ component, given $\eta = 1$ and the modal estimates $(\hat{\beta}, \hat{\rho}^2, \hat{\theta}, \hat{\tau}^2, \hat{\sigma})$, falls below a threshold of 0.5. This gives rise to a reduced model space consisting of 2^{p^*} models, where $p^* \leq p$, based on the design matrix X^* with p^* columns from the original design matrix X corresponding to the included covariates. When the true data generating model contains substantially fewer signals than p , the resulting reduced model space facilitates better mixing and greater stability of the Gibbs sampler compared with the one operating in the original model space. Accordingly, the reduced model space is utilized in the Gibbs sampling step (Step 2) of our proposed algorithm.

Step 2: The Gibbs Sampling Step

In the second step, we study the tail behavior and perform uncertainty quantification through an MCMC algorithm on the reduced model space deduced from the ECM-based modal estimates. The likelihood and priors in (3) corresponding to the stochastic search HEM (De and Ghosh, 2026) enable closed-form full conditional distributions, which can be further utilized to deduce an efficient Gibbs sampler, along with an MH-step to address model selection. Although a preliminary level of model reduction is performed in the ECM step, we incorporate this additional step of model uncertainty on the reduced model space to allow dropping of any potential false positives/signals. Moreover, the flexibility in tail is induced through a discrete uniform prior on the shape parameter

η , as indicated in (3).

2.3 Choice of Hyperparameters

The proposed GECM-HEM algorithm involves several hyperparameters, whose choices are crucial to the performance of the algorithm. For the ECM step, a vital question arises regarding the choice of κ_0 and κ_1 in the prior on the regression coefficients β in (5). Conditional on τ^2 , κ_0 and κ_1 respectively controls the variances of the spike and the slab components. Similarly, marginalization over τ^2 leads to a mixture of multivariate Student- t priors on β with λ_τ degrees of freedom, and scale parameters $\kappa_0\rho^2$ and $\kappa_1\rho^2$ corresponding to the spike and the slab components respectively. In this case, κ_0 and κ_1 regulates the scales of the respective Student- t distributions in the spike and the slab components. Besides, the prior specification in (3) yields a multivariate Student- t prior with λ_τ degrees of freedom and scale ρ^2 on the non-zero regression coefficients β_γ in the Gibbs sampling step, when marginalized over τ^2 . Since the covariates and response variables are standardized, we choose $\kappa_1 = 1$, which also preserves consistency between the priors on the slab components in the ECM and the Gibbs sampling steps. Furthermore, we take $\lambda_\tau = 1$ for reasonably thick tailed priors on the slab components.

The spike hyperparameter κ_0 affects the algorithm even more critically than the slab. Rather than suggesting a single value, it is more appealing to tune κ_0 from a grid of values, based on the data. Following the grid recommended by [Ročková and George \(2014\)](#), we allow κ_0 to be selected from $\{0.01, 0.02, \dots, 0.51\}$ through 10-fold cross-validation. The optimal κ_0 is chosen to be the value which minimizes the median of the fold-wise medians of absolute differences between the actual and the predicted values of the response variables. It might be noted that the cross-validation can be carried out in parallel to enhance the computational efficiency of the algorithm.

Since the response variables are standardized to have a unit variance, an $\text{InvGamma}(a_\rho = 2.1, b_\rho = 0.1)$ prior is placed on the hyperbolic error scale parameter ρ^2 , such that the prior mass is mostly concentrated below one. For θ , the probability of the slab component, we consider a $\text{Beta}(r_\theta = 1, s_\theta = 1)$ prior, which has also been widely used in the literature.

The role of the shape parameter η of the hyperbolic errors requires some discussion as well. As indicated in Section 2.2, the value of η is considered to be fixed at the ECM step, while associating a prior to it in the Gibbs sampler. That is, η serves as a fixed hyperparameter for the ECM step and as a vital parameter with a prior in the Gibbs sampling step. Ideally, putting a prior on η throughout the entire algorithm would have been more appropriate for capturing tail uncertainty. However, owing to the inability of suitable tail estimation by the ECM, as observed in preliminary analyses, the value of η is fixed at $\eta = 1$. It might be noted that the normal and the Laplace distributions can be obtained as limiting cases of the hyperbolic distribution for large and small values of η respectively. A value of $\eta = 1$ produces tails heavier than those of a normal distribution but much lighter than those of a Laplace distribution. When the degree of tail heaviness is unknown and cannot be accurately estimated, this choice represents a practical compromise and may reduce sensitivity to model misspecification. For the Gibbs sampling step, we put a discrete uniform prior on η with prior support $\mathcal{G}_\eta = \{0.05, 0.1, 0.2, 0.3, \dots, 0.9, 1, 2, 5, 10, 20, 50\}$, as suggested by De and Ghosh (2026), to study the unknown tail behavior more extensively.

3 Simulation Study

The efficacy of the proposed GECM-HEM technique is demonstrated through simulation studies in comparison with several competing methods. We generate $n = 400$ observations from the regression model

$$y_i = \beta_0 + \beta_1 x_{i1} + \beta_2 x_{i2} + \dots + \beta_p x_{ip} + \epsilon_i, \quad i = 1, 2, \dots, n, \quad (12)$$

under the following scenarios:

- (I) We take $p = 1000$. The covariates $\mathbf{x}_i = (x_{i1}, x_{i2}, \dots, x_{ip})^\top$, $i = 1, 2, \dots, n$, are independently drawn from a multivariate normal distribution $N_p(\mathbf{0}, \Sigma_X)$ with a first order autoregressive correlation structure as $\Sigma_X = (0.6^{|k-l|})_{1 \leq k, l \leq p}$. The true regression coefficients are

$\beta_0 = 2, \beta_1 = \dots = \beta_{100} = 1.5, \beta_{101} = \dots = \beta_p = 0$. The errors are assumed to follow a Hyperbolic($\eta = 0.5, \rho^2 = 2$) distribution.

(II) This scenario is similar to Scenario (I), except that the errors are normally distributed with zero mean and variance 2.

(III) Here, we take $p = 1500$, and the covariates x_{ij} s ($i = 1, 2, \dots, n; j = 1, 2, \dots, p$) are independently drawn from a standard normal distribution. The true regression coefficients are $\beta_0 = 2, \beta_1 = \dots = \beta_{50} = 1.5, \beta_{51} = \dots = \beta_p = 0$, and the errors have a Student- t distribution with 2.05 degrees of freedom.

(IV) With $p = 1500$ and a design matrix similar to Scenario (III), we consider the true regression coefficients as $\beta_0 = 2, \beta_1 = \dots = \beta_{50} = 0.9, \beta_{51} = \dots = \beta_p = 0$, and generate errors from a Hyperbolic($\eta = 0.5, \rho^2 = 2$) distribution.

Each scenario is replicated 100 times to capture variability in the resulting performance measures. The studied methods are assessed in terms of estimation and out-of-sample predictive performances. For studying estimation performance, we consider the root-mean-squared errors (RMSEs) of the regression coefficients, defined as $\left[(p+1)^{-1} \sum_{j=0}^p (\beta_j - \hat{\beta}_j)^2 \right]^{1/2}$, where $\hat{\beta}_j$ denotes the estimate of the j th regression coefficient β_j ($j = 0, 1, 2, \dots, p$). We also compare the RMSEs of the expected values of the response variables, $\mathbb{E}(y_i | \boldsymbol{\beta}) = \sum_{j=0}^p \beta_j x_{ij}$, obtained as $\left[n^{-1} \sum_{i=1}^n \left\{ \sum_{j=0}^p x_{ij} (\beta_j - \hat{\beta}_j) \right\}^2 \right]^{1/2}$, where $x_{i0} = 1$, for every $i = 1, 2, \dots, n$. Moreover, the true positive rates (TPRs) and the true negative rates (TNRs) of the methods are examined to inspect the variable selection performance. The TPR denotes the proportion of signals correctly identified by a method among all the true signals, while the TNR is the proportion of correctly dropped noise variables among all the true noise variables. Therefore, both TPR and TNR should be equal to 1 in an ideal scenario of perfect detection of signals and noise variables. Based on 1000 out-of-sample observations for each scenario, the predictive performance is evaluated using median of absolute differences (MeADs) between the actual and the predicted values of the response variables, as well as empirical coverage probabilities and median widths of 90% prediction intervals.

3.1 Comparison With the Stochastic Search HEM

At the outset, we demonstrate the advantage of GECHM-HEM over the usual stochastic search HEM (G-HEM) (De and Ghosh, 2026) in Section 2.1 for large model spaces, using the simulation setting in Scenario (I) with hyperbolic errors. Our goal is to highlight the computational benefits of posterior exploration in a reduced model space using GECHM-HEM, compared to exploration by G-HEM in the entire model space containing all the 2^p models.

For a thorough investigation, G-HEM is executed with two different model initialization schemes for the MCMC algorithm. Specifically, G-HEM-Null starts the posterior exploration from a null model with no covariates by setting $\gamma = \mathbf{0}$ and $\beta = \mathbf{0}$, whereas G-HEM-Full begins the MCMC at the full model containing all covariates, with $\gamma_j = 1$ ($j = 1, 2, \dots, p$) and β set to the corresponding ridge estimate. For the proposed GECHM-HEM procedure, model selection is first performed using the ECM step (with cross-validation implemented on four CPU cores), after which the Gibbs sampling is implemented under the reduced model for 11000 iterations, discarding the first 1000 iterations as burnin. In a similar amount of clock time, G-HEM-Full runs for 1000 iterations (after a burnin of 100), while G-HEM-Null runs for 4000 iterations (after a burnin of 1000).

Because of the robustness of median over mean, the point estimates $(\hat{\beta}_1, \hat{\beta}_2, \dots, \hat{\beta}_p)^\top$ of the regression coefficients $(\beta_1, \beta_2, \dots, \beta_p)^\top$ are taken as the component-wise medians of the posterior samples. Moreover, for every MCMC iteration, the posterior samples of $(\beta_1, \beta_2, \dots, \beta_p)^\top$ lead to a draw of the intercept parameter β_0 as

$$\beta_0 = \bar{Y} - \sum_{j=1}^p \beta_j \bar{x}_j, \quad (13)$$

where \bar{Y} is the mean of the non-centered and unscaled response variable, and \bar{x}_j is the mean of the non-centered and unscaled j th covariate ($j = 1, 2, \dots, p$). The posterior median $\hat{\beta}_0$ of these MCMC samples provides a point estimate of β_0 . Similarly, MCMC samples for the expected values of the response variables, $\mathbb{E}(y_i|\beta)$ s ($i = 1, 2, \dots, n$), are obtained at every iteration using

the posterior samples of $(\beta_0, \beta_1, \beta_2, \dots, \beta_p)^\top$ as

$$\mathbb{E}(y_i|\boldsymbol{\beta}) = \beta_0 + \sum_{j=0}^p \beta_j x_{ij}, \quad (14)$$

and their posterior medians serve as the corresponding point estimates. Using these estimates, the RMSEs of the regression coefficients as well as those of the expected response variables are computed and compared through boxplots in Figure 1. Both the plots in Figure 1 depict significantly lower RMSEs for the proposed GECHM-HEM method than for the G-HEM versions, with G-HEM-Full as the closest competitor.

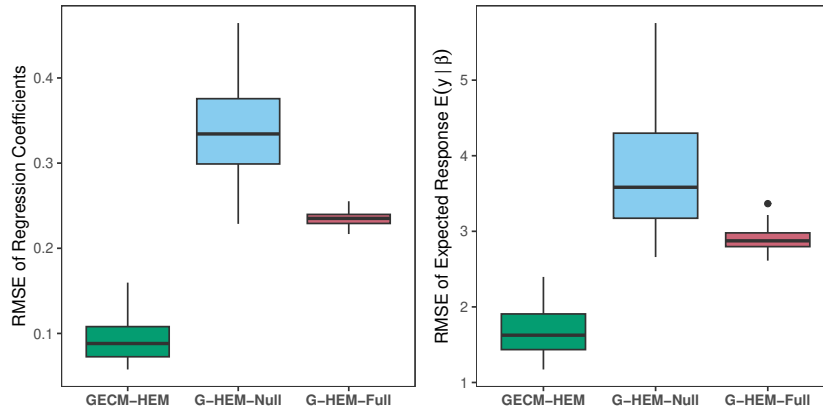


Figure 1: RMSEs of all regression coefficients and the expected values of the response variables for the proposed GECHM-HEM method and different versions of G-HEM under true hyperbolic errors in Scenario (I). The boxplots are based on 100 replicates.

To assess the efficacy of GECHM-HEM for variable selection, we examine the inclusion indicators γ_{js} ($j = 1, 2, \dots, p$), which are estimated using the median probability model (Barbieri and Berger, 2004). More precisely, the j th inclusion indicator is estimated as $\hat{\gamma}_j = 1$, if the corresponding marginal posterior inclusion probability $\mathbb{P}(\gamma_j = 1|\mathbf{Y})$ is at least 0.5. The estimated inclusion indicators are used to calculate the TPRs and TNRs against the true inclusion indicators, and the results are summarized in Table 1. G-HEM-Null yields low values of both TPR and TNR through incorrect identification of most of the signals and noise variables. Likewise, G-HEM-Full remains entrapped at the full model throughout the MCMC chain and fails to drop any covariate, as evident from its TPR of 1 and TNR of 0. In contrast, with both TPR and TNR values close to 1, our method

GECM-HEM shines in inclusion and exclusion of appropriate variables.

Table 1: TPRs and TNRs of all covariates for the proposed GECM-HEM method and different versions of G-HEM under true hyperbolic errors in Scenario (I). The values are averaged over 100 replications.

	GECM-HEM	G-HEM-Null	G-HEM-Full
TPR	0.990	0.682	1.000
TNR	0.999	0.815	0.000

We now proceed to compare the predictive performance of the three methods with a newly generated test dataset of 1000 observations and the estimates from the training samples. Using the MCMC samples based on the training set, we obtain the point predictions for the test samples and compute their MeADs from the actual values of the response variables. For uncertainty quantification, we use the estimated quantiles of the posterior predictive distributions to construct 90% prediction intervals, and measure their empirical coverage probabilities and median widths. All the results, based on 100 replications, pertaining to predictive performance are presented in Figure 2. GECM-HEM performs satisfactorily in terms of point prediction. As far as prediction intervals are concerned, GECM-HEM attains nominal coverage, while the two versions of G-HEM show substantial overcoverage with significantly larger median widths.

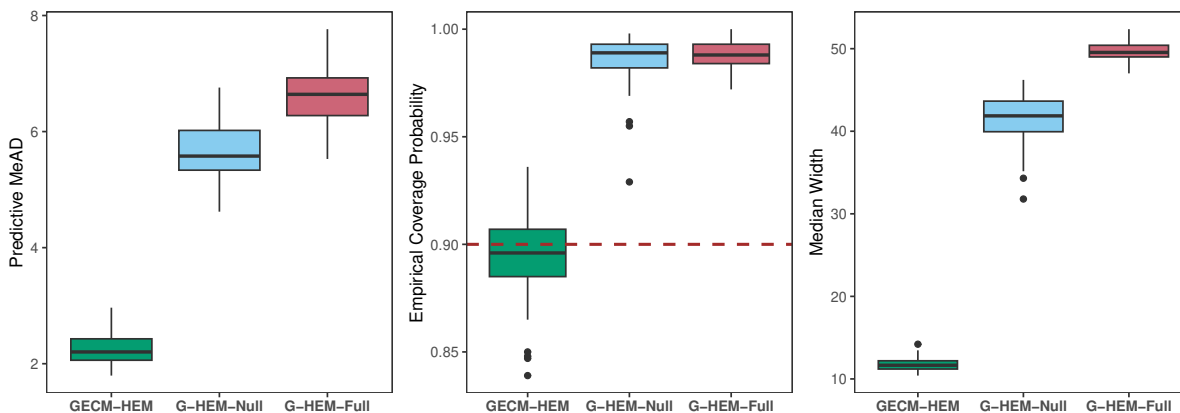


Figure 2: Predictive performance of the proposed GECM-HEM method and different versions of G-HEM under true hyperbolic errors in Scenario (I). In the middle plot, the dashed line marks a coverage of 90%. The boxplots are based on 100 replicates.

To summarize, GECM-HEM remarkably outperforms G-HEM in coefficient estimation, variable selection and prediction, in the same running time. Thus, for large model spaces, performing

MCMC on a posterior mode guided reduced model space appears to be a more computationally efficient alternative to a traditional implementation of MCMC-based posterior exploration over the entire model space.

3.2 Comparison With MAP Estimators

In this section our goal is to compare the performance of GECM-HEM with two state-of-the-art MAP estimation techniques, namely, EMVS (Ročková and George, 2014) and SSQLASSO (Liu et al., 2024). Under different kinds of spike-and-slab priors, both the contenders perform deterministic model selection through posterior maximization using the EM algorithm. Specifically, the EMVS algorithm assumes a normal likelihood, while SSQLASSO incorporates a heavier-tailed asymmetric Laplace likelihood. The competing models thus enable a two-fold comparison. First, the study helps us scrutinize the potential advantages and disadvantages of our proposed hybrid approach over MAP estimators. Second, we can compare the flexibility of different likelihoods in capturing tail-heaviness. For the present analysis, SSQLASSO and EMVS are implemented using the `emBayes` (Liu and Wu, 2024) and `EMVS` (Ročková and Moran, 2021) packages in R respectively.

At first, we evaluate the methods in terms of estimation of the regression coefficients and the expected values of the response variables. For GECM-HEM, these are estimated using the respective posterior medians, as stated in Section 3.1. On the other hand, the MAP techniques estimate the same quantities via posterior maximization. From the boxplots of the RMSEs of the regression coefficients in Figure 3, GECM-HEM typically shows the lowest RMSEs among the three methods for the normal and the Student- t error models, while exhibiting competitive performance with SSQLASSO for true hyperbolic errors. EMVS consistently produces the largest RMSEs across all the scenarios, with hyperbolic errors depicting the most stark difference with the other two. A similar observation can be made for the expected responses $\mathbb{E}(\mathbf{y}|\boldsymbol{\beta})$ from the boxplots of their RMSEs in Figure 3.

We now refer to the TPRs and TNRs of the methods in Table 2 to analyze their variable selec-

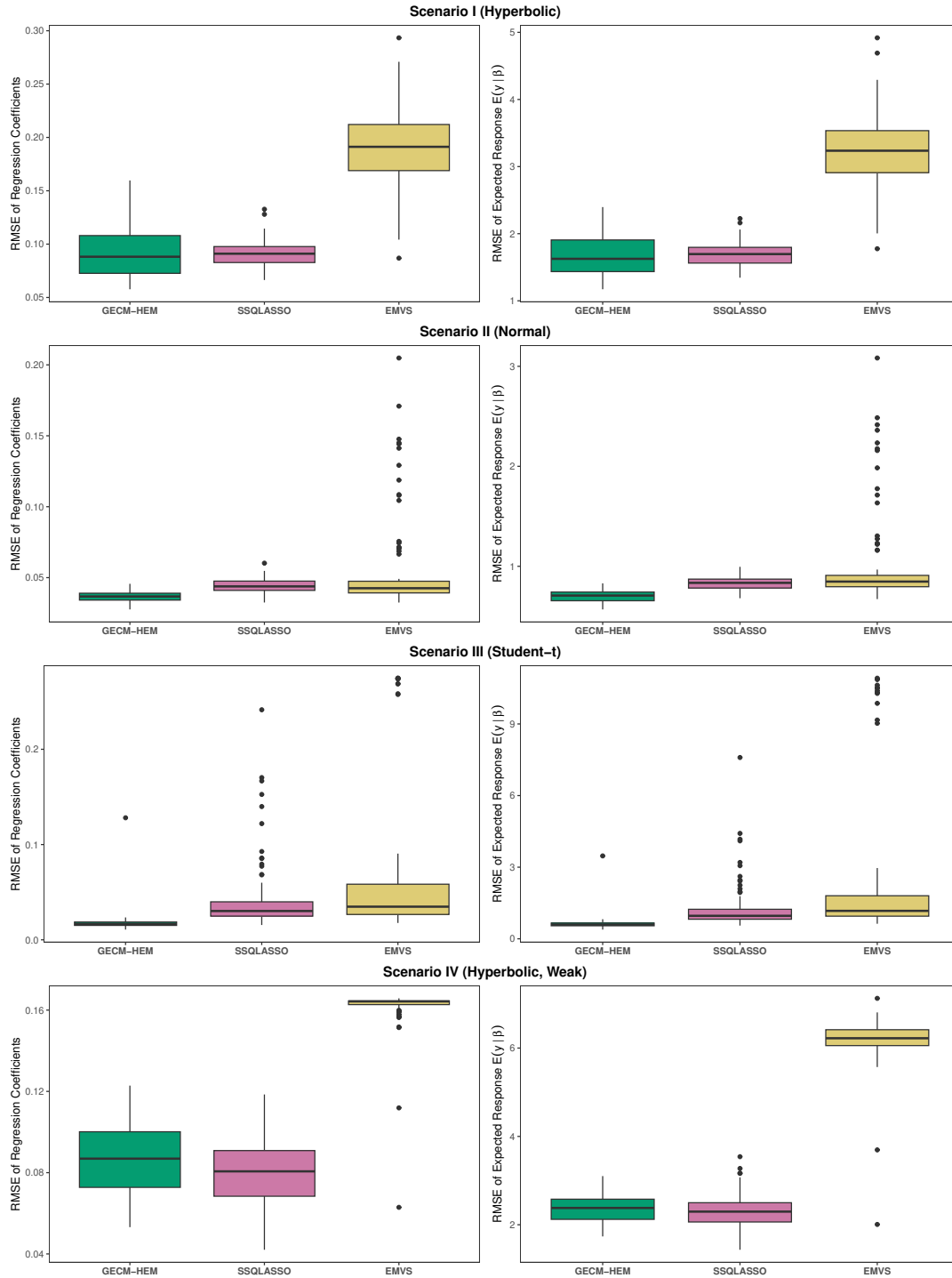


Figure 3: RMSEs of all regression coefficients and the expected values of the response variables for the proposed GECM-HEM method and the other studied MAP-based methods under different scenarios. The boxplots are based on 100 replications.

tion performance. Similar to Section 3.1, variable selection for GECM-HEM is carried out using the median probability model (Barbieri and Berger, 2004). On the other hand, for the MAP-based methods EMVS and SSQLASSO, we use the models returned by their respective R packages. Under Scenarios (I)-(III), the TPRs and TNRs for GECM-HEM are close to 1, indicating the effectiveness of our proposed method in including signals and excluding noise covariates. For Scenario (IV), corresponding to signals with smaller magnitudes and accordingly weaker information, we observe a drop in both the metrics for GECM-HEM, with the reduction being less pronounced for the TNR. SSQLASSO produces similar TPRs but lower TNRs than GECM-HEM across all the scenarios, while EMVS shows the reverse pattern with similar TNRs and lower TPRs. In other words, SSQLASSO and EMVS favor larger and smaller models respectively, while our method tends to make a trade-off, with a slight preference towards smaller models.

Table 2: TPRs (TNRs) of all regression coefficients for the proposed GECM-HEM method and the other studied MAP-based methods under different scenarios. The values are averaged over 100 replications.

	GECM-HEM	SSQLASSO	EMVS
Scenario (I) (Hyperbolic)	0.990 (0.999)	1.000 (0.956)	0.895 (1.000)
Scenario (II) (Normal)	1.000 (1.000)	1.000 (0.707)	0.993 (1.000)
Scenario (III) (Student- t)	0.999 (0.998)	0.993 (0.947)	0.893 (0.998)
Scenario (IV) (Hyperbolic, Weak)	0.916 (0.973)	0.912 (0.944)	0.031 (1.000)

Next, we look at the prediction results in Figure 4. The predictive MeAD behaves similarly to the RMSEs of the regression coefficients and the mean response in Figure 3. That is, in terms of point prediction, GECM-HEM shows competitive performance with SSQLASSO, with slight improvement for the normal and the Student- t generating models. EMVS is consistently outperformed by yielding larger MeAD values than the other two methods. We also study the prediction intervals for the methods based on the out-of-sample observations. For GECM-HEM, the predictions are carried out using the posterior predictive distribution. For SSQLASSO and EMVS, the predictive errors are generated from their respective assumed error distributions, that is, Laplace for SSQLASSO and normal for EMVS, conditional on the obtained posterior modes. As far as prediction intervals are concerned, the results in Figure 4 exhibit two distinct patterns: one for Scenario

(IV) and another for Scenarios (I)-(III). In Scenario (IV), with weaker signals than in the remaining scenarios, all the methods display undercoverage. While the undercoverage is most severe for EMVS, the coverage for SSQLASSO is more variable than GECM-HEM. The corresponding widths of the prediction intervals behave similarly to the coverage, with the shortest intervals for EMVS and more varying widths for SSQLASSO. For Scenarios (I) and (II) corresponding to hyperbolic and normal errors, SSQLASSO has a general tendency of significant undercoverage with shorter widths compared to GECM-HEM, while EMVS produces wider intervals than GECM-HEM with notable overcoverage. In these scenarios, GECM-HEM attains nominal coverage. Under Student- t errors in Scenario (III), the three methods exhibit similar widths and maintain a coverage close to the nominal level.

In a nutshell, GECM-HEM exhibits competitive performance in coefficient estimation and point prediction, and superior performance in variable selection and uncertainty quantification through prediction intervals. Moreover, the consistency of the results for GECM-HEM across the scenarios indicates its robustness to different error distributions. However, the comparatively modest performance of GECM-HEM in Scenario (IV), corresponding to low signal strength, suggests that simultaneous tail estimation and variable selection may require stronger signals.

3.3 Computation Time

We conclude the simulation study by highlighting the computational advantage of our proposed method. Both the competing methods EMVS and SSQLASSO are implemented in C through their respective software packages, whereas our method is executed in R. Therefore, the computation times may not be strictly comparable, since lower level programming languages such as C are generally faster than higher level languages such as R. Despite this fact, we investigate the potential gain of using parallel computation to perform cross-validation for choosing the optimal value of the spike hyperparameter in the ECM step of our proposed method, which is a distinctive feature of our algorithm.

The computation times of the algorithms are reported in Table 3. For GECM-HEM, we run

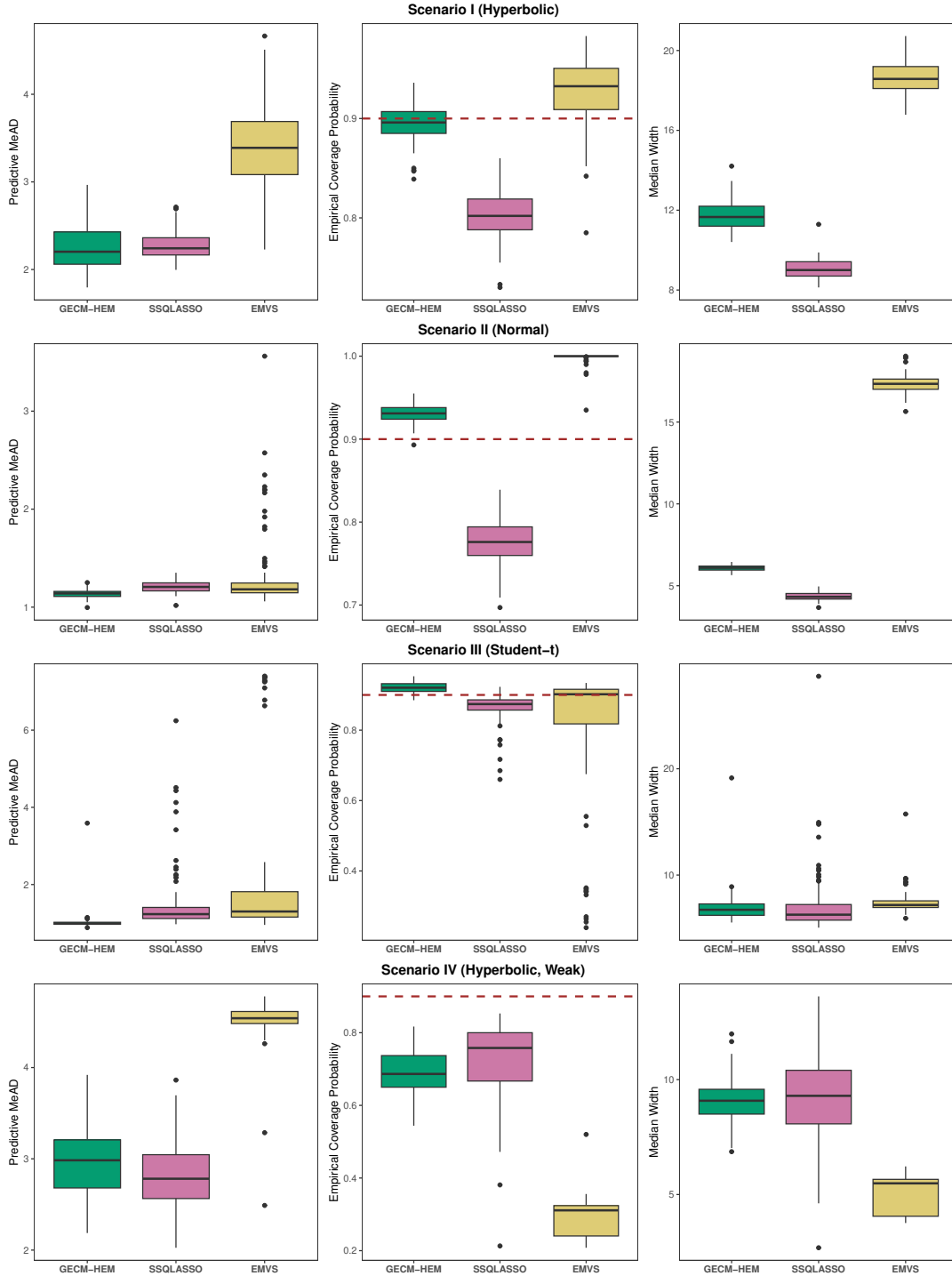


Figure 4: Predictive performance of the proposed GECM-HEM method and the other studied MAP-based methods under different scenarios. The boxplots are based on 100 replications.

the method using 1, 4, 6 and 10 CPU cores respectively. Since any standard computer typically consists of 4 or 6 CPU cores, we choose these values to study the time taken by the proposed

method in a traditional machine. The remaining choices, namely 1 and 10 cores, correspond to no parallelization and parallelization over a larger number of cores than in a standard machine respectively. We observe from Table 3 that while EMVS turns out to be the fastest among the three methods, GECHM-HEM is computationally competitive with SSQLASSO and can be made faster through parallel computation, even though SSQLASSO is implemented in C while GECHM-HEM is implemented in R. Overall, our proposed GECHM-HEM method appears to be a computationally viable alternative for simultaneous tail estimation, variable selection and uncertainty quantification, compared to state-of-the-art MAP-based techniques.

Table 3: Computation time (in minutes) for the proposed GECHM-HEM method using different number of CPU cores, and the other MAP-based methods, under a single replication of Scenario I with errors generated from hyperbolic distribution.

GECHM-HEM				SSQLASSO	EMVS
1 core	4 cores	6 cores	10 cores		
23.50	11.65	10.23	6.23	21.87	1.60

4 Real Data Analysis

We now proceed to demonstrate the performance of GECHM-HEM using three real datasets. Every dataset is divided into training and test sets with a 90%-10% split ratio, and the process is repeated 100 times to reduce sensitivity of the results to a specific choice of split. Our proposed method is compared with EMVS and SSQLASSO in terms of predictive accuracy through median absolute deviations of the predicted test sample response values, empirical coverage probabilities and median widths of 90% prediction intervals. The results on predictive accuracy are depicted in Figure 5. Additionally, we inspect model parsimony across the methods for each dataset. It is worthwhile to mention that for our proposed GECHM-HEM method, the variable selection is carried out using the median probability model (Barbieri and Berger, 2004), similar to the simulation study in Section 3.

4.1 Boston Housing Dataset

The Boston Housing dataset from the `MASS` package in R, which has been extensively used as a benchmark example for regression modeling with heavy-tailed errors, is used as an illustrative example in this paper. It consists of 506 observations on median house value, regressed on 13 neighborhood characteristics as covariates. To achieve an approximate symmetry in the distribution of the residuals, the logarithm of the median house value is considered as the response variable. Following [Ghosh and Reiter \(2013\)](#); [De and Ghosh \(2024, 2026\)](#), we add 1000 noise variables, independently generated from a standard normal distribution, resulting in $p = 1013$, to make the problem more interesting for variable selection. This enables us to compare how effectively the competing methods can drop the noise variables from the model, which can in turn affect the predictive performance.

From the boxplots in the topmost panel in [Figure 5](#), we observe that while SSQLASSO typically yields the lowest predictive MeAD values, GECCM-HEM is a close competitor. On the other hand, in terms of empirical coverages and median widths of 90% prediction intervals, both GECCM-HEM and SSQLASSO usually attain nominal coverage, with slightly wider intervals for GECCM-HEM. EMVS is outperformed by the other two methods in all aspects, with larger predictive MeAD, substantial undercoverage, and overly narrow prediction intervals. In other words, GECCM-HEM exhibits satisfactory performance in uncertainty quantification through prediction intervals and a competitive performance in point prediction.

We now investigate the model size chosen by each method. The design matrix is known to contain 1000 noise variables, along with the 13 original predictors. With this information up front, it will be useful to study these two types of covariates separately. In particular, for each type, we look at the five-number summary statistics of the number of covariates included in the model. The summaries are taken over the 100 replicates and are reported in [Table 4](#). It is evident from [Table 4](#) that for most of the replicates, all the three methods perform similarly in choosing the original covariates and dropping the noise variables. However, we also observe that SSQLASSO includes nearly all of the original covariates and retains a large number of noise predictors in some

replicates, indicating its tendency to choose bigger models.

Table 4: Five-number summary statistics of the number of covariates (original and noise) included in the model by the proposed GECM-HEM method and the other studied MAP-based methods for the Boston Housing dataset. The statistics are computed based on 100 replications.

Covariates	Method	Minimum	1st Quartile	Median	3rd Quartile	Maximum
Original (13)	GECM-HEM	3	4	4	5	5
	SSQLASSO	3	4	4	5	12
	EMVS	3	3	3	3	5
Noise (1000)	GECM-HEM	0	0	0	1	3
	SSQLASSO	0	0	0	0	819
	EMVS	0	0	0	0	2

4.2 University of Vermont Faculty Salaries Dataset

We analyze data on faculty salaries for the year 2020 at the University of Vermont obtained from Kaggle, using the log-transformed salary as the response variable, with job title, department and college serving as predictors. Furthermore, since all the 3 covariates are categorical with multiple levels, we create dummy variables for each level, and also incorporate the interactions between colleges and job titles. The resulting dataset consists of 1756 observations, with 936 covariates and the logarithm of salary as the response variable.

It is to be noted that 605 of the interaction terms are not observed in the data. Accordingly, these 605 columns in the design matrix contain only zero entries across all rows. Instead of removing these columns manually, we retain them to check if the studied methods can effectively discard them. We observe that while GECM-HEM and EMVS can successfully exclude these columns, the implementation of SSQLASSO via the `emBayes` package results in a runtime error. Therefore, we execute SSQLASSO on the smaller design matrix containing the remaining 331 columns, after manually dropping the 605 columns with all zero entries.

The middle panel of Figure 5 shows the predictive performance of the methods. Similar to the Boston Housing dataset, the predictive MeADs for GECM-HEM and SSQLASSO are close to one another, with slightly lower values for SSQLASSO, while those for EMVS are substantially larger.

All the methods exhibit undercoverage for 90% prediction intervals. The proposed GECHM-HEM method attains a coverage nearly similar to that of EMVS, but with a smaller width. On the other hand, SSQLASSO produces narrower intervals and notably lower coverage than the other methods.

To compare model sizes, we examine the number of predictors selected by each method among the 331 covariates used in fitting SSQLASSO. A quick glance at the five-number summaries in Table 5 reveals a sharp distinction in the model sparsity across the methods. Both EMVS and GECHM-HEM favor smaller models, with EMVS selecting the least number of covariates. In contrast, SSQLASSO exhibits limited shrinkage by dropping only a few covariates in most replicates.

Table 5: Five-number summary statistics of the number of covariates (among the 331 covariates used to run SSQLASSO) included in the model by the proposed GECHM-HEM method and the other studied MAP-based methods for the Faculty Salaries dataset. The statistics are computed based on 100 replications.

Method	Minimum	1st Quartile	Median	3rd Quartile	Maximum
GECHM-HEM	22	27	28	29	33
SSQLASSO	87	319	323	325	328
EMVS	5	5	5	5	5

4.3 Ames Housing Dataset

As an alternative to the Boston Housing dataset, [De Cock \(2011\)](#) proposed the Ames Housing dataset (available in the `modeldata` package in R) as a touchstone for heavy-tailed regression modeling problems. The original dataset contains 2930 observations on 74 variables, including house price and 73 covariates potentially affecting the prices. To capture potential nonlinear effects, we create bins for some of the numeric covariates, thereby converting them to categorical variables. In particular, we consider 12 bins each for the year of building a house and the year of its remodeling. Thereafter, we include interaction terms between the neighborhood, and year of building, year of remodeling and year of sale (considered to be categorical with sale years as levels). Using dummy variables for each level of the categorical variables, the resulting design

matrix consists of 2930 rows and 962 columns, and the log-transformed selling price is taken as the response variable.

In this example, SSQLASSO can be successfully executed for only 11 out of the 100 replicates using the `emBayes` package in R. Therefore, we report our findings for the three methods based on these 11 replicates in the main paper, and specify the results for GECHM-HEM and EMVS based on all the 100 replicates in Appendix B. Using the 11 replicates, the boxplots in Figure 5 indicate slightly lower MeAD for SSQLASSO than GECHM-HEM. The prediction intervals for GECHM-HEM are a bit wider and show a slight overcoverage, compared to a slight undercoverage by SSQLASSO. Both the methods significantly outperform EMVS, which yields large predictive MeAD, along with wide prediction intervals and gross undercoverage.

The variable selection results (Table 6) based on the 11 replicates repeats a similar story like the Faculty Salaries dataset. EMVS chooses the smallest model, followed by GECHM-HEM, while SSQLASSO retains a substantial number of predictors.

Table 6: Five-number summary statistics of the number of covariates included in the model by the proposed GECHM-HEM method and the other studied MAP-based methods for the Ames Housing dataset. The statistics are computed based on 11 replications for which SSQLASSO can be successfully executed.

Method	Minimum	1st Quartile	Median	3rd Quartile	Maximum
GECHM-HEM	36	38	39	41	44
SSQLASSO	827	922	929	947	955
EMVS	7	10	14	15	15

5 Conclusion

In this paper, we have proposed a two-step approach, namely, GECHM-HEM, by combining MAP estimation through the ECM algorithm, along with a Gibbs sampler, for performing model selection and posterior computation within a heavy-tailed framework. This approach leverages the computational advantage of MAP estimation and inferential benefits of MCMC-based algorithms. Compared with two representative MAP estimators and a stand-alone MCMC-based approach,

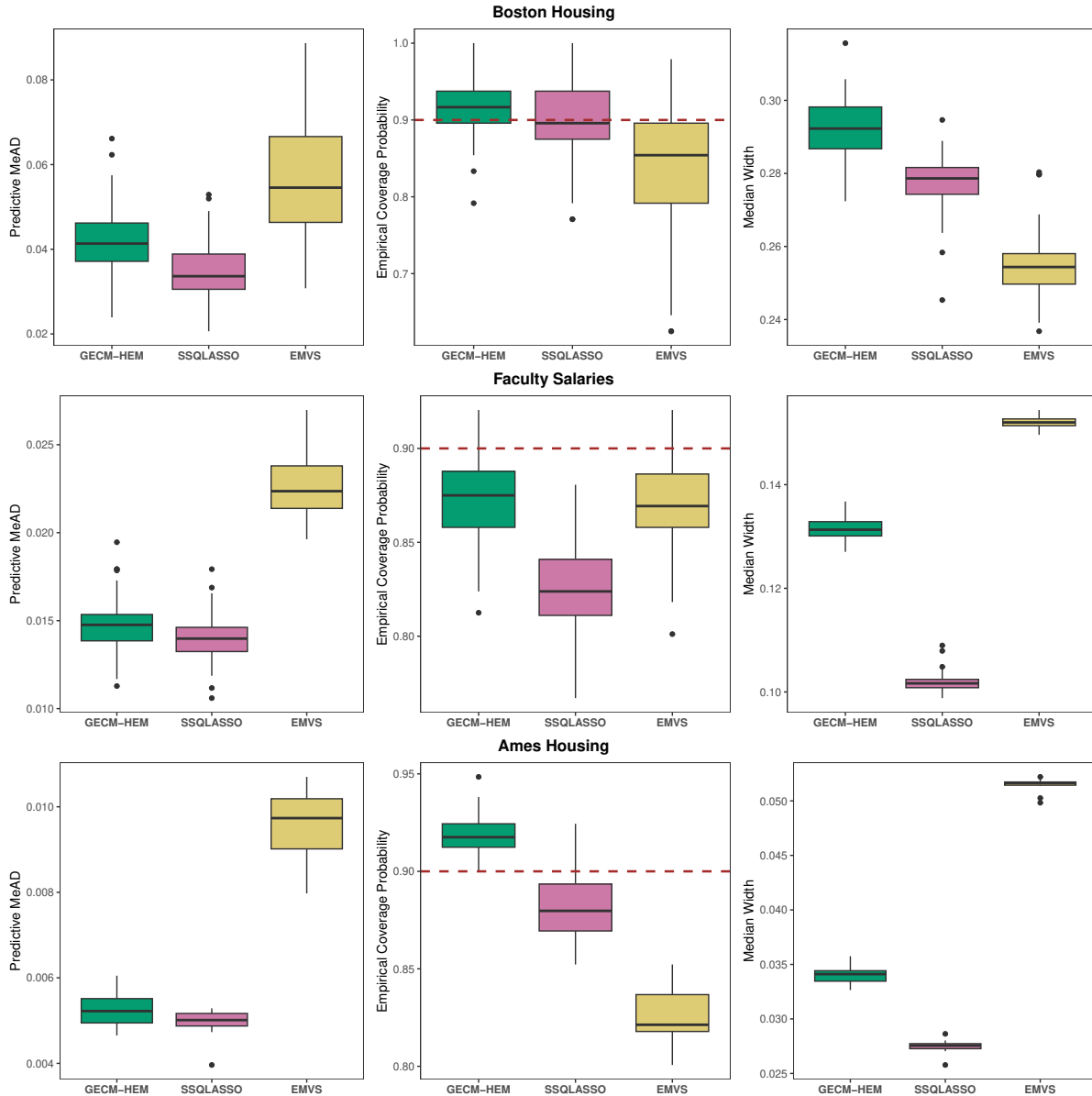


Figure 5: Predictive performance of the proposed GECHM-HEM method and the other studied MAP-based methods for different real datasets. In the plots for empirical coverage probability, the dashed lines mark a coverage of 90%. The boxplots for Boston Housing and Faculty Salaries datasets are based on 100 replications. The boxplots for Ames Housing dataset are based on 11 replications for which SSQ LASSO can be successfully executed.

the proposed GECHM-HEM method has shown competitive performance in coefficient estimation and point prediction, and has demonstrated superior performance in variable selection and uncertainty quantification. Although for a fixed degree of tail-heaviness, MAP-based techniques like SSQ LASSO can produce more precise estimates, our method performs favorably in simultane-

ously accommodating tail flexibility and uncertainty quantification.

We conclude this paper with some possible directions for future work. Unlike [De and Ghosh \(2026\)](#), we have focused solely on the hyperbolic distribution rather than a mixture of hyperbolic and Student- t distributions for modeling errors. [Fernandez and Steel \(1999\)](#) pointed out the potential asymptotic unboundedness of the Student- t likelihood, and cautioned against using likelihood maximization techniques such as EM-like algorithms for this distribution when the degrees of freedom are small. A possible future direction is to extend our proposed GECM-HEM technique to the mixture of hyperbolic and Student- t errors ([De and Ghosh, 2026](#)), with careful specification of the prior for the tail heaviness parameter. Furthermore, studying the Bayesian bootstrap ([Rubin, 1981](#); [Nie and Ročková, 2023a,b](#)) as an alternative to the Gibbs sampler for uncertainty quantification in the second step of our proposed method is another possibility. Lastly, instead of using spike-and-slab priors on regression coefficients with beta-binomial priors on the model size, exploring alternative priors like the horseshoe prior ([Carvalho et al., 2009, 2010](#); [De and Ghosh, 2024](#)) and the recently proposed matryoshka doll prior ([Womack et al., 2025](#); [Ghosh, 2025](#)) represents another possible direction for future work.

References

- Barbieri, M. and Berger, J. (2004). Optimal predictive model selection. *The Annals of Statistics*, 32(3):870–897.
- Carvalho, C., Polson, N., and Scott, J. (2009). Handling sparsity via the horseshoe. In van Dyk, D. and Welling, M., editors, *Proceedings of the Twelfth International Conference on Artificial Intelligence and Statistics*, volume 5 of *Proceedings of Machine Learning Research*, pages 73–80. PMLR.
- Carvalho, C., Polson, N., and Scott, J. (2010). The horseshoe estimator for sparse signals. *Biometrika*, 97(2):465–480.

- Chakraborty, S., Khare, K., and Michailidis, G. (2025). A generalized Bayesian approach for high-dimensional robust regression with serially correlated errors and predictors. *arXiv preprint, arXiv:2412.05673*.
- Clyde, M., Ghosh, J., and Littman, M. (2011). Bayesian adaptive sampling for variable selection and model averaging. *Journal of Computational and Graphical Statistics*, 20(1):80–101.
- De, S. and Ghosh, J. (2024). Horseshoe prior for Bayesian linear regression with hyperbolic errors. *Statistics and Applications*, 22(3):199–209.
- De, S. and Ghosh, J. (2026). Robust Bayesian model averaging for linear regression models with heavy-tailed errors. *Journal of Applied Statistics*, 53(2):304–330.
- De Cock, D. (2011). Ames, Iowa: Alternative to the Boston Housing data as an end of semester regression project. *Journal of Statistics Education*, 19(3):1–15.
- Dempster, A., Laird, N., and Rubin, D. (1977). Maximum likelihood from incomplete data via the EM algorithm. *Journal of the Royal Statistical Society: Series B (Methodological)*, 39(1):1–22.
- Fernandez, C. and Steel, M. (1999). Multivariate Student-t regression models: Pitfalls and inference. *Biometrika*, 86(1):153–167.
- George, E. and McCulloch, R. (1993). Variable selection via Gibbs sampling. *Journal of the American Statistical Association*, 88(423):881–889.
- George, E. and McCulloch, R. (1997). Approaches for Bayesian variable selection. *Statistica Sinica*, 7(2):339–373.
- Ghosh, J. (2025). On the choice of model space priors and multiplicity control in Bayesian variable selection: an application to streaming logistic regression. *arXiv preprint arXiv:2512.22504*.
- Ghosh, J. and Clyde, M. (2011). Rao-Blackwellization for Bayesian variable selection and model averaging in linear and binary regression: A novel data augmentation approach. *Journal of the American Statistical Association*, 106(495):1041–1052.

- Ghosh, J. and Ghattas, A. (2015). Bayesian variable selection under collinearity. *The American Statistician*, 69(3):165–173.
- Ghosh, J. and Reiter, J. (2013). Secure Bayesian model averaging for horizontally partitioned data. *Statistics and Computing*, 23(3):311–322.
- Gneiting, T. (1997). Normal scale mixtures and dual probability densities. *Journal of Statistical Computation and Simulation*, 59(4):375–384.
- Gramacy, R. and Pantaleo, E. (2010). Shrinkage regression for multivariate inference with missing data, and an application to portfolio balancing. *Bayesian Analysis*, 5(2):237–262.
- Hans, C. (2010). Model uncertainty and variable selection in Bayesian lasso regression. *Statistics and Computing*, 20:221–229.
- Hans, C. (2011). Elastic net regression modeling with the orthant normal prior. *Journal of the American Statistical Association*, 106(496):1383–1393.
- Liu, Y., Ren, J., Ma, S., and Wu, C. (2024). The spike-and-slab quantile LASSO for robust variable selection in cancer genomics studies. *Statistics in Medicine*, 43(26):4928–4983.
- Liu, Y. and Wu, C. (2024). *emBayes: Robust Bayesian Variable Selection via Expectation-Maximization*. R package version 0.1.6.
- Meng, X.-L. and Rubin, D. (1993). Maximum likelihood estimation via the ECM algorithm: A general framework. *Biometrika*, 80(2):267–278.
- Nie, L. and Ročková, V. (2023a). Bayesian bootstrap spike-and-slab lasso. *Journal of the American Statistical Association*, 118(543):2013–2028.
- Nie, L. and Ročková, V. (2023b). Deep bootstrap for Bayesian inference. *Philosophical Transactions of the Royal Society A: Mathematical, Physical and Engineering Sciences*, 381(2247):20220154.

- Park, T. and Casella, G. (2008). The Bayesian lasso. *Journal of the American Statistical Association*, 103(482):681–686.
- Ren, J., Zhou, F., Li, X., Ma, S., Jiang, Y., and Wu, C. (2023). Robust bayesian variable selection for gene–environment interactions. *Biometrics*, 79(2):684–694.
- Ročková, V. and George, E. (2014). EMVS: The EM approach to Bayesian variable selection. *Journal of the American Statistical Association*, 109(506):828–846.
- Ročková, V. and George, E. (2018). The spike-and-slab lasso. *Journal of the American Statistical Association*, 113(521):431–444.
- Ročková, V. and Moran, G. (2021). *EMVS: Bayesian Variable Selection using EM Algorithm*. R package version 1.2.1.
- Rubin, D. (1981). The Bayesian bootstrap. *The Annals of Statistics*, 9(1):130–134.
- Ruth, W. (2024). A review of Monte Carlo-based versions of the EM algorithm. *arXiv preprint, arXiv:2401.00945*.
- Wei, G. and Tanner, M. (1990). A Monte Carlo implementation of the EM algorithm and the poor man’s data augmentation algorithms. *Journal of the American Statistical Association*, 85(411):699–704.
- Womack, A., Taylor-Rodríguez, D., and Fuentes, C. (2025). The matryoshka doll prior – principled multiplicity correction in Bayesian model comparison. *Bayesian Analysis*, pages 1–25.
- Zanella, G. and Roberts, G. (2019). Scalable importance tempering and Bayesian variable selection. *Journal of the Royal Statistical Society: Series B (Statistical Methodology)*, 81(3):489–517.

Appendix A Proof of Proposition 1

Proposition 1. Let A and a be random variables such that $A|a^2 \sim N(0, \rho^2 a^2)$ and $a^2 \sim \text{GIG}(1, \eta, \eta)$. Then A is distributed as $\text{Hyperbolic}(\eta, \rho^2)$.

Proof. The conditional density of A given a^2 is

$$f_A(A|a^2) = \frac{1}{\sqrt{2\pi\rho^2 a^2}} \exp\left(-\frac{A^2}{2\rho^2 a^2}\right), \quad -\infty < A < \infty,$$

while the density of a^2 is

$$f_{a^2}(a^2) = \frac{1}{2K_1(\eta)} \exp\left\{-\frac{\eta}{2}\left(a^2 + \frac{1}{a^2}\right)\right\}, \quad x > 0.$$

The density of A , marginalized over a^2 , is obtained as

$$\begin{aligned} f_A(A) &= \int_0^\infty f_A(A|a^2) f_{a^2}(a^2) da^2, \\ &= \frac{1}{2K_1(\eta)\sqrt{2\pi\rho^2}} \int_0^\infty \frac{1}{\sqrt{a^2}} \exp\left\{-\frac{1}{2}\left(\eta a^2 + \frac{\eta + A^2/\rho^2}{a^2}\right)\right\} da^2. \end{aligned}$$

The above integral can be evaluated using the $\text{GIG}(\lambda, a, b)$ kernel in (15) with $\lambda = 1/2$, $a = \eta$, $b = \eta + A^2/\rho^2$, thereby yielding

$$f_A(A) = \frac{1}{\sqrt{2\pi\rho^2}K_1(\eta)} \left(\frac{\eta + A^2/\rho^2}{\eta}\right)^{1/4} K_{1/2}\left(\sqrt{\eta(\eta + A^2/\rho^2)}\right),$$

which further simplifies to the density function of the $\text{Hyperbolic}(\eta, \rho^2)$ distribution in (2), using the closed form expression $K_{1/2}(x) = \sqrt{\pi/2x} e^{-x}$. \square

Appendix B Additional Results for Ames Housing Dataset

In this section, we reproduce the results for GECHM-HEM and EMVS based on all the 100 replicates intended for our analysis. The results on both predictive performance (Figure 6) and model size

(Table 7) for the methods are nearly similar to those stated in Section 4.3, with GECHM-HEM visibly outperforming EMVS in every aspect of comparison.

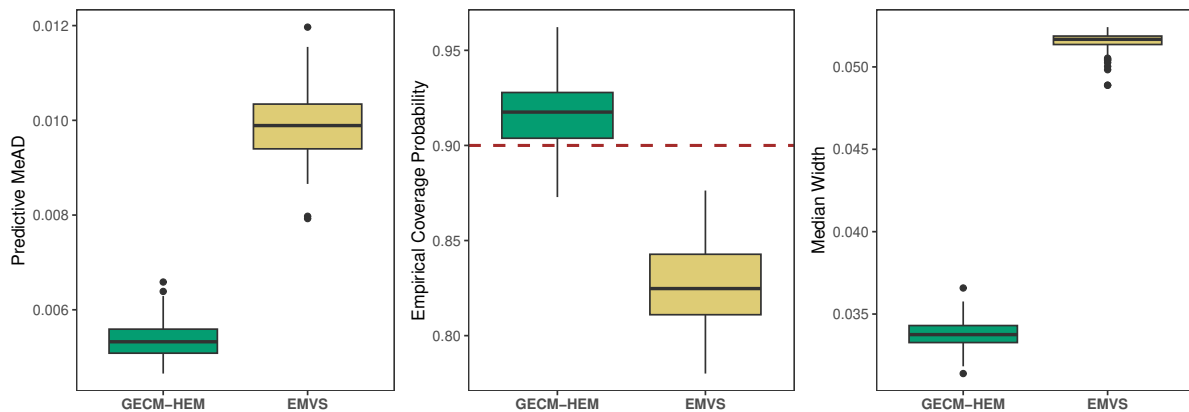


Figure 6: Predictive performance of the proposed GECHM-HEM method and EMVS for Ames Housing dataset. In the middle plot, the dashed line marks a coverage of 90%. The boxplots are based on 100 replications.

Table 7: Five-number summary statistics of the number of covariates included in the model by the proposed GECHM-HEM method and EMVS for the Ames Housing dataset. The statistics are computed based on 100 replications.

Method	Minimum	1st Quartile	Median	3rd Quartile	Maximum
GECHM-HEM	33	38	40	41	59
EMVS	3	13	14	14	16

Appendix C Some Useful Distributions

Some of the frequently encountered probability distributions in this article are reviewed in this section, to remove ambiguity about the parameterizations of their density functions used herein.

1. The generalized inverse Gaussian (GIG) distribution, denoted by $GIG(\lambda, a, b)$, has a density

$$f_{GIG}(x|\lambda, a, b) = \frac{(a/b)^{\lambda/2}}{2K_{\lambda}(\sqrt{ab})} x^{\lambda-1} e^{-(ax+b/x)/2}, \quad x > 0, \quad (15)$$

where $a, b > 0, \lambda \in \mathbb{R}$ and K_{λ} is a modified Bessel function of the second kind.

2. The density function of the gamma distribution $\text{Gamma}(a, b)$ is

$$f_{\text{Gamma}}(x|a, b) = \frac{b^a}{\Gamma(a)} x^{a-1} e^{-bx}, \quad x > 0, \quad (16)$$

where $a > 0$ and $b > 0$ are the shape and the rate parameters respectively.

3. Similarly, the inverse gamma distribution $\text{InvGamma}(a, b)$ has the density

$$f_{\text{InvGamma}}(x|a, b) = \frac{b^a}{\Gamma(a)} x^{-a-1} e^{-b/x}, \quad x > 0, \quad (17)$$

where $a > 0$ and $b > 0$ respectively denote the shape and the scale parameters.

4. The probability mass function of the discrete uniform distribution $\text{DiscUniform}(\mathcal{G})$ on a finite set of real values \mathcal{G} can be expressed as

$$f_{\text{DiscUniform}}(x) = \frac{1}{|\mathcal{G}|}, \quad x \in \mathcal{G}, \quad (18)$$

where $|\mathcal{G}|$ represents the number of elements in \mathcal{G} .